Available online at www.sciencedirect.com
ScienceDirect
Journal of Marine Systems 74 (2008) 978–993
JOURNAL OF MARINE SYSTEMS
www.elsevier.com/locate/jmarsys

Picophytoplankton and nanophytoplankton abundance and distribution in the southeastern Beaufort Sea (Mackenzie Shelf and Amundsen Gulf) during Fall 2002

Irene R. Schloss [a,*,1], Christian Nozais [b], Sébastien Mas [a], Bon van Hardenberg [c], Eddy Carmack [c], Jean-Éric Tremblay [d], Sonia Brugel [a], Serge Demers [a]

[a] *Institut des sciences de la mer de Rimouski, 310 Allée des Ursulines, Rimouski (Qc), Canada G5L 3A1*
[b] *Laboratoire d'écologie des systèmes aquatiques, Département de biologie, chimie et géographie, Université du Québec à Rimouski, 300 Allée des Ursulines, Rimouski (Qc), Canada G5L 3A1*
[c] *Department of Fisheries and Oceans, Institute of Ocean Sciences, 9860 West Saanich Road, Sidney B.C., Canada V8L 4B2*
[d] *Département de biologie, Pavillon Alexandre-Vachon, local 2056A, Université Laval Québec, Canada G1K 7P4*

Received 7 March 2007; received in revised form 15 November 2007; accepted 21 January 2008
Available online 5 February 2008

Abstract

The distribution of picophytoplankton (0.2–2 μm) and nanophytoplankton (2–20 μm) in the Beaufort Sea–Mackenzie Shelf and Amundsen Gulf regions during autumn, 2002 is examined relative to their ambient water mass properties (salinity, temperature and nutrients: nitrate + nitrite, phosphate, and silicate) and to the ratio of variable to maximum fluorescence, Fv/Fm. Total phytoplankton and cell abundances (<20 μm) were mainly correlated with salinity. Significant differences in picophytoplankton cell numbers were found among waters near the mouth of the Mackenzie River, ice melt waters and the underlying halocline water masses of Pacific origin. Picophytoplankton was the most abundant phytoplankton fraction during the autumnal season, probably reflecting low nitrate concentrations (surface waters average ~0.65 μM). The ratio Fv/Fm averaged 0.44, indicating that cells were still physiologically active, even though their concentrations were low (max Chl a=0.9 mg m^{-3}). No significant differences in Fv/Fm were evident in the different water masses, indicating that rate limiting conditions for photosynthesis and growth were uniform across the whole system, which was in a pre-winter stage, and was probably already experiencing light limitation as a result of shortening day lengths.

Keywords: Beaufort Sea; Mackenzie River; Water masses; Picophytoplankton; Nanophytoplankton; Fv/Fm, Chlorophyll fluorescence

1. Introduction

Arctic shelves comprise roughly 50% of the area of the Arctic Ocean, and the biological and biogeochemical processes that occur on these shelves dominate the carbon cycle (see Stein and Macdonald, 2004). Primary

* Corresponding author.
E-mail address: Irene.Schloss@uqar.qc.ca (I.R. Schloss).
[1] Permanent address: Instituto Antártico Argentino, Cerrito 1248, C1010AAZ, Buenos Aires, Argentina, and CONICET, Argentina.

0924-7963/$ - see front matter © 2008 Elsevier B.V. All rights reserved.
doi:10.1016/j.jmarsys.2008.01.004

production on arctic shelves varies greatly from region to region, from season to season and from year to year in response to differences in ice (e.g., concentration, thickness, duration), riverine input (e.g., nutrients, particles) and ocean forcing (e.g. through flow, upwelling, wind and tidal mixing; Carmack et al., 2006). Recent years have witnessed a dramatic decrease in sea ice extent (Stroeve et al., 2005) and the major fraction of this reduction has in fact taken place in the Beaufort Sea (Shimada et al., 2006). It is also predicted that the quantity and timing of river discharge to the Arctic Ocean will change as climate warms (Peterson et al., 2006). The Mackenzie Shelf and adjacent Amundsen Gulf region of the southeastern Beaufort Sea are thus critically located in the context of climate variability (Carmack and Macdonald, 2002).

The Mackenzie Shelf in the Beaufort Sea is delimited to the west by Mackenzie Canyon, to the north by the Canada Basin, to the east by Amundsen Gulf and to the south by the Mackenzie River Delta (Carmack et al., 2004). In the coastal margins of arctic shelves, landfast sea ice is formed annually (Barber and Hanesiak, 2004). Seasonality in the region is not only influenced by annual sea ice formation but also by the inflow of fresh water from several rivers, by far the largest of which is the Mackenzie River. Inflow from the Mackenzie River onto the shelf contributes to the shelf's freshwater and the dissolved and particulate organic matter (Parsons et al., 1988).

The oceanography of the Southern Canada Basin and the Mackenzie Shelf has been documented in several studies (see synthesis in Carmack and Macdonald, 2002). Briefly, waters from several origins can be identified and, other than the influence of Mackenzie River, waters on the shelf and surface waters in the Beaufort Sea are of Pacific Ocean origin (McLaughlin et al., 1996, 2004), while waters at depth (>200 m) originate in the Atlantic Ocean (Macdonald et al., 1989). The clockwise Beaufort Gyre dominates the movement of sea ice and surface water. Below the surface water, the flow reverses to counter-clockwise forming the so-called Beaufort Undercurrent, moving waters of both Pacific and Atlantic origin eastward along the continental margin, providing nutrients to shelf waters. The relationship of such environmental factors to the temporal and spatial distribution of phytoplankton on arctic shelves remains, however, poorly understood. Typically, studies having good seasonal coverage give limited spatial range, while those with large spatial coverage have poor temporal resolution.

One of the aims of the CASES (Canadian Arctic Shelf Exchange Study) project is to study the temporal variation in the major water properties in the Beaufort Sea. A first expedition was undertaken in September–October 2002, during the period of minimum ice extent (Parkinson et al., 1999). The hypothesis that the Mackenzie River subsidizes to a great extent the pool of planktonic cells of the Beaufort Sea has been tested in several previous works (Galand et al., 2006; Garneau et al., 2006; Lovejoy et al., 2006, 2007; Waleron et al., 2007). We here present a snap-shot of picophytoplankton (0.2–2 μm) and nanophytoplankton (2–20 μm) distributions analysed by means of flow cytometry in an area heavily influenced by riverine input. We examine their relationships to ambient water mass properties (temperature, salinity, nutrients) in order to find out whether and riverine influence could be tracked in the area by means of phytoplankton (<20 μm) distribution. We further discuss plankton physiological state during Fall 2002 by means of the maximum photochemical yield measured by fluorescence.

2. Materials and methods

CASES 2002 was conducted from September 23 to October 14, 2002, on board the CCGS *Pierre Radisson.* 37 sampling stations were occupied in the Beaufort Sea, from the mouth of the Mackenzie River to Amundsen Gulf, and to the ice edge in the Canadian Basin (Fig. 1). For the determination of nutrients, phytoplankton biomass and composition, water samples were collected with a rosette sampler (SBE Carrousel), equipped with 24 12-L PVC bottles (Ocean Test Equipment Inc) and prefiltered on 330 μm mesh to remove large grazers.

Samples were taken at the optical depths as determined with a Secchi disk, corresponding to 100, 40, 20, 10, 5, 1 and 0.1% PAR. Optical depths were calculated considering the Secchi depth = 1.7 K_d (following Koenings and Edmundson, 1991) where K_d is the PAR vertical attenuation coefficient for downwelling irradiance, which was used to estimate the mentioned optical depths according to Kirk (1983). This is a crude visual method that could certainly entrain a large error, especially in the estimation of 0.1% irradiance. Downwelling cosine corrected photosynthetically-available radiation (PAR) were obtained with a PAR sensor attached to the CTD (High pressure connector) Biospherical Inst. QCP-2300L (cosine). A QCR-2200 (Biospherical Inst.) sensor measured surface irradiance.

Inorganic nutrient concentrations (nitrate + nitrite, phosphate and silicate) were determined on board on fresh samples with an ALPKEM Autoanalyser with routine colorimetric techniques (Grasshoff, 1999) and an analytical detection limit of 0.05 μmol L^{-1} for nitrate

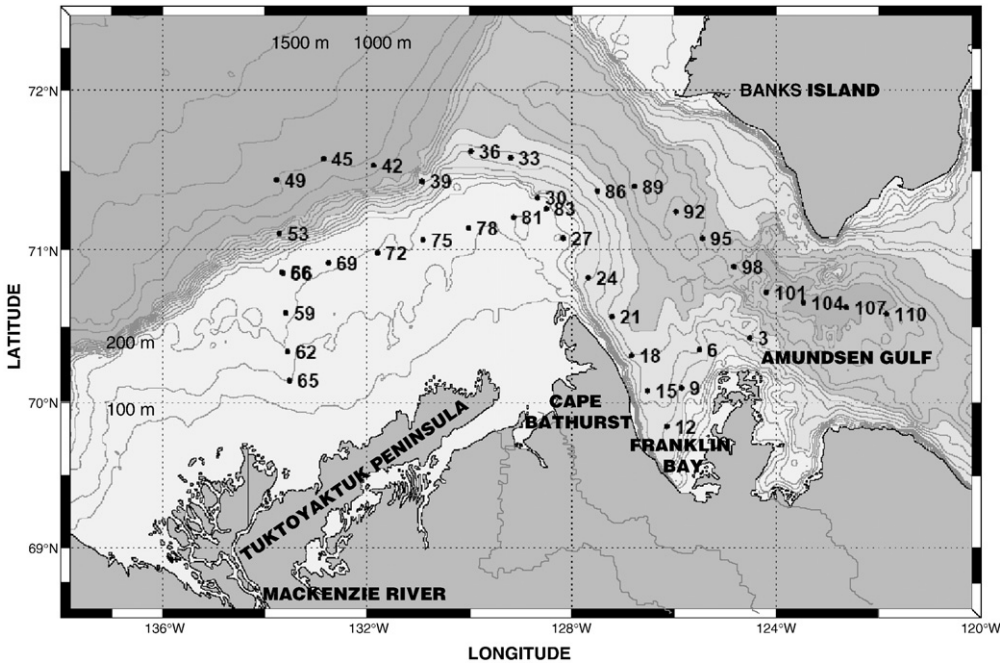

Fig. 1. Map of the southeastern Beaufort Sea showing the location of sampling stations.

and phosphate, and 0.1 μmol L^{-1} for silicate. Total chlorophyll *a* (Chl *a*), a proxy for phytoplankton biomass, was determined on water samples (250 to 1000 mL) filtered onto Whatman GF/F filters (total Chl *a*) and onto 5 μm polycarbonate (Poretics) filters (Chl *a* >5 μm). Chl *a* concentrations of both fractions were measured using a 10-AU Turner Designs fluorometer following 24 h extraction in 90% acetone at 4 °C without grinding (Parsons et al., 1984).

For the determination of picophytoplankton (<2 μm diameter) and nanophytoplankton (2–20 μm) cell abundance, 4.5-mL subsamples were preserved with paraformaldehyde (2% final concentration), as recommended by Troussellier et al. (1995), and stored at −80 °C for later analysis in the laboratory. Fluorescent cells were counted using a FACSORT Analyser flow cytometer (FCM, Becton Dickinson, San Jose, CA, equipped with a 488 nm laser beam of 15 mW). The FCM simultaneously measured cell concentration determined from the pump flow rate (60 μL min^{-1}) and sample run time (2 to 10 min) along with cell properties such as forward angle scatter (size index) and cell red fluorescence (FL3>650 nm) were documented. The latter is attributed to chlorophyll *a*, and allows the detection of phytoplankton. The forward light scatter signals were calibrated using Fluoresbrite beads (Polyscience Inc., Warrington, PA) of different sizes. For all samples, two 2-mL replicates were analysed following the addition of beads of 2, 10 and 20 μm as internal standard of size. The data were logged and analysed using Cell Quest and Attractors software (both from Becton Dickinson), respectively.

Fluorescence measurements were conducted on water samples using an Optisciences Pulse-Amplitude Modulated (PAM) fluorometer (model OS5-FL, Opti-Sciences, Inc., Tyngsboro, Massachusetts, USA). In this pulse modulated fluorometer chlorophyll fluorescence is excited with a narrow bandwidth source centered at 660 nm, and detected in the 710–750 nm range. For the detection of the 690 fluorescence peak, a source centered at 450 nm is resent. High intensity white light (350 and 700 nm) saturates the photosystem, and a 685 nm source is used to drive photosynthetic activity.

For each station, a blank was first determined on sea water sampled at that same station filtered onto Whatman GF/F filters. Then, the photochemical quantum yield of photosystem II (PSII) reaction centers (Fv/Fm) was determined in dark-acclimated phytoplankton (45 min). Fv results from the difference between the maximum fluorescence, Fm, reached under a strong saturating pulse of white light irradiance, when all reaction centers of PSII are closed (reduced) and the initial sample fluorescence F_0, when all reaction centers of PSII are open (oxidized). The Fv/Fm ratio was used as an indicator for the potential (or maximal) of electron flow through PSII in the dark-adapted state (Falkowski and Raven, 1997).

In order to study the relationships between the different measured variables, Spearman's rank correlation coefficients were calculated. Nonparametric correlation was preferred to parametric correlation because the numbers of observations of the various parameters were different. A complete linkage clustering of a matrix of Euclidean distances among the standardized temperature and salinity data was used with the aim of grouping and comparing the different sampling points (stations and depths) in the TS diagram (see Fig. 2). Then, after testing for the assumptions of the analysis of variance (ANOVA; normality and homocedacy) a 1-way ANOVA was performed in order to search for significant differences in biological parameters (Chl *a*, picophytoplankton and nanophytoplankton cell concentrations and the Fv/Fm ratio) among water masses. Post-hoc comparisons were performed with Tukey's Honestly Significant Differences test for unequal sample sizes using the Statistica Software (Statsoft).

3. Results

The water masses of the study area are shown in Fig. 2. The Mackenzie River plume (MR) is characterised by high temperatures (between 0.4 and 1 °C) and very low salinities (between 16 and 20). These waters mix with cool, ice melt waters (IM) from both land and sea origin to form the surface layer. Winter waters (WW) lie immediately below these waters and are identified by salinities <30 and temperatures ~ −0.5 °C. Both Pacific Summer Water (PSW), which is identified by a subsurface temperature maximum at depths between 30 and 40 m, and Pacific Winter Water (PWW), which is identified by a relatively thick temperature maximum at depth ~80–120 m are clearly recognized (Fig. 2). Lower Halocline Waters (LHW), with salinities near 34.4 and temperatures near −1 °C, lie between PWW and Atlantic Water (AW), at depths greater than about 200 m, are characterised by their higher temperatures (~0.5 °C) and salinities (between 34.6 and 34.9).

Near surface temperature (at depth <10 m) varied with station location and ranged between −1.6 and 1.0 °C. Fig. 3A shows that warmer surface waters were present near the mouth of the Mackenzie River, cooling across the Mackenzie shelf towards Amundsen Gulf. Temperatures were lower in the vicinity of the shelf break near 71 °N. Salinity in surface waters further reflected the distance to the coast, reflecting patterns of rivers discharging low-salinity waters into the shelf area (Fig. 3B). Temperature decreased and salinity increased from the Mackenzie Shelf northward. At greater depths, both temperature and salinity were closely aligned with topography, reflecting the regional circulation (data not shown).

Surface irradiance at local noon ranged from 127 to 536 μmol photons m^{-2} s^{-1}. Surface waters (<10 m) diffuse attenuation coefficient for downwelling PAR (K_d) ranged from 0.07 to 0.3 m^{-1}.

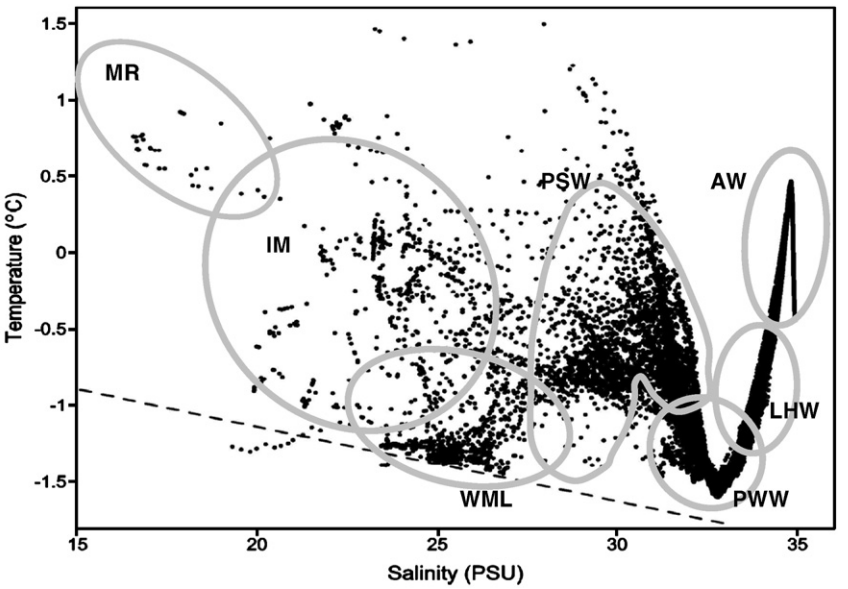

Fig. 2. T/S correlation diagram showing water masses found in the study area: MR is Mackenzie River; IM is ice melt water; WML is the Winter Mixed Layer; PSW is Pacific Summer Water; PWW is Pacific Winter Water; LHW is Lower Halocline Water; and AW is Atlantic Water. The dashed line indicates the freezing temperatures.

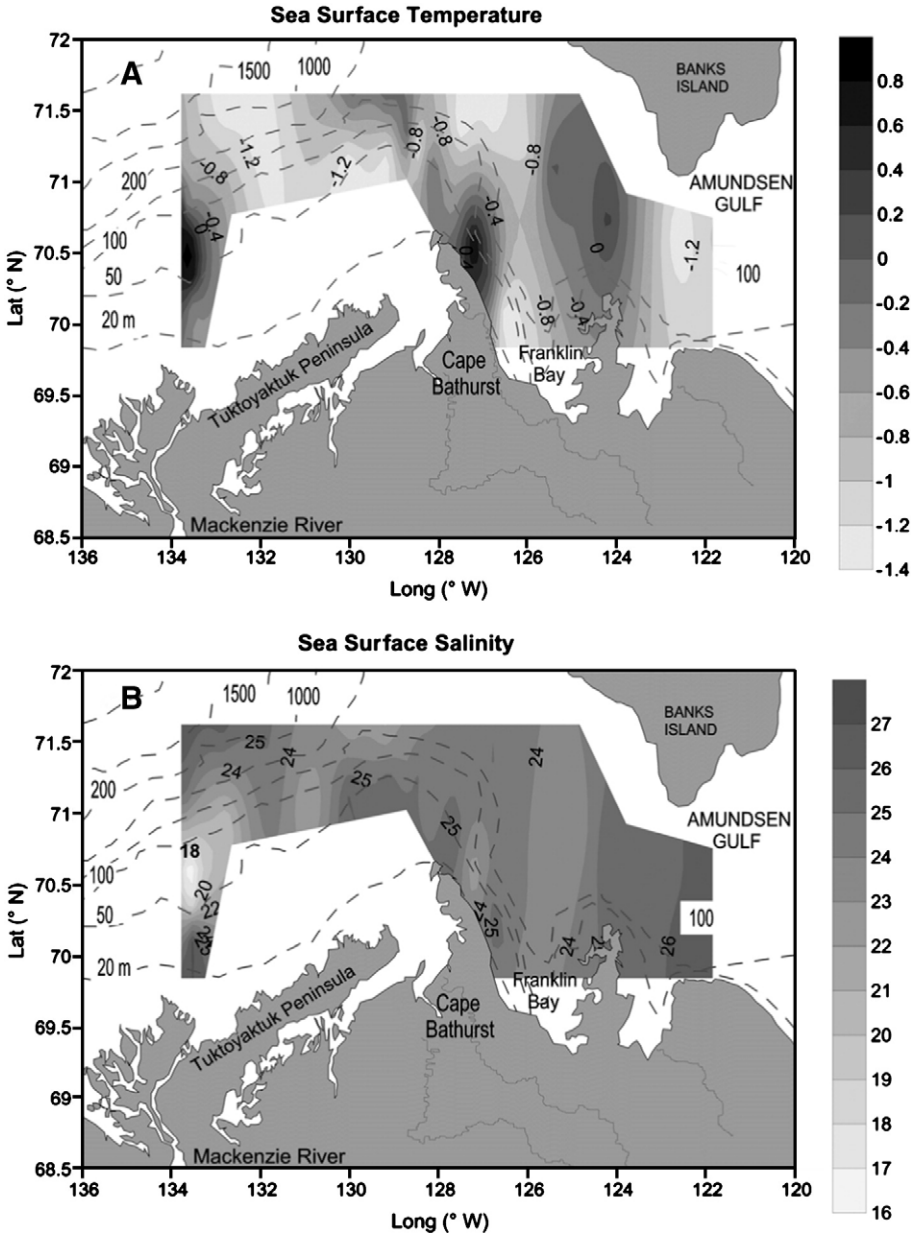

Fig. 3. Horizontal distribution of average A) temperature and B) salinity for surface waters (0–10 m).

Nitrate + nitrite and silicate concentrations (Fig. 4A) ranged from undetectable values (surface waters of Stn 33) to 17 μM (Stn 98, at 150 m); in the stations closest to the Mackenzie River mouth nitrate was around 0.4 μM, both in surface and below it. Phosphate concentrations ranged from 0.1 to 2.62 μM, although surface concentrations were always <0.5 μM (Fig. 4B). Molar nitrate + nitrite/phosphate (N:P) ratio for all depths was 4.62 (±0.32). Considering only surface waters, the ratio was 1.15 and 1.76 for depths <10 and between 10 and 50 m, respectively. Silicates varied between 0.2 (surface waters, Stn 18) and 39.4 μM (Stn 89, at 150 m), but concentrations were around 26 μM below 50 m depth in the coastal shelf. A similar deep increase in silicate was observed in the offshore stations, some of the rich silicate water extending over the shelf (data not shown).

The average Chl *a* value for the whole area was 0.23 (±0.32) mg Chl *a* m^{-3}. Significant differences ($p<0.05$) were found in Chl *a* concentrations between depths. Maximum values were found at Stn 6 (0.93 mg Chl *a* m^{-3}) (Fig. 5), and in general in surface waters (<10 m;

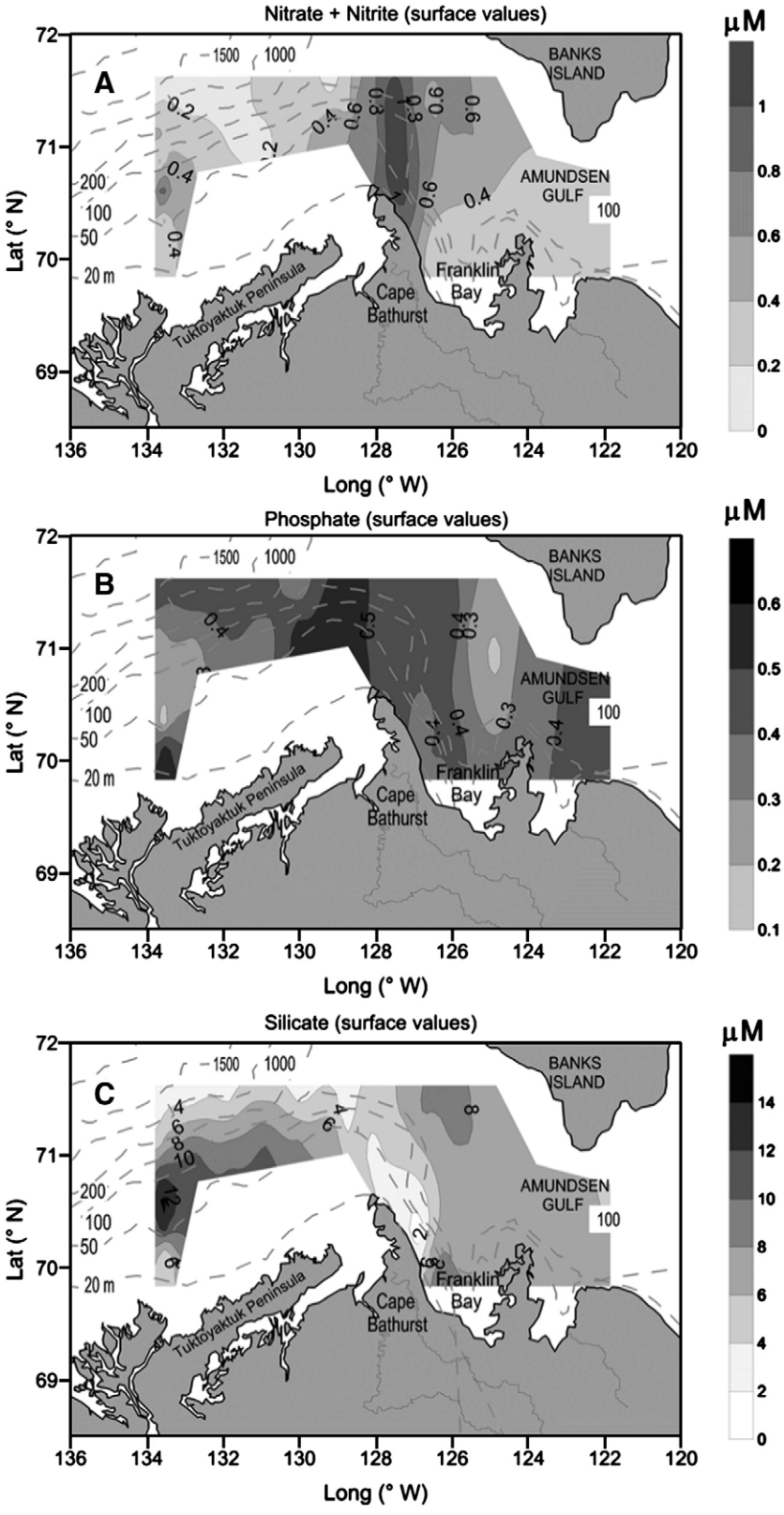

Fig. 4. Surface (0–10 m) average values of A) Nitrate + Nitrite, B) Phosphate and C) Silicate observed in the study area.

(0.46±0.03 mg Chl *a* m^{-3}), followed by the intermediate water depths (between 10 and 50 m, 0.20±0.11 mg Chl *a* m^{-3}). At depths >50 m, Chl *a* concentration averaged 0.08±0.11 mg Chl *a* m^{-3}. In offshore stations (Stns 36 to 49) Chl *a* maxima (around 0.2 mg Chl *a* m^{-3}) were found between 40 m and 60 m (Fig. 5A). Fractionated Chl *a* showed that most of this pigment was due to cells <5 μm (Fig. 5B). The highest Chl *a* >5 μm value (0.49 mg Chl *a* m^{-3}) was found in Stn 42, in the outer shelf, at 59 m, exceptionally representing almost 70% of the Chl *a*. In most of the stations, the proportion of Chl *a* >5 μm varied between 5 and 25% of total Chl *a*. The lowest Chl *a* values were found in most coastal areas – i.e. in the stations influenced by the Mackenzie River (stations 65 and 62), in Stn 18, in the vicinities of Cape Bathurst – and typically at greater depths in all stations.

Picophytoplankton were the main component of the phytoplankton assemblages (<20 μm) in most of the stations and depths. Picophytoplankton cell concentrations were significantly higher in surface waters, above 10 m, than at deeper depths ($p<0.05$). In coincidence

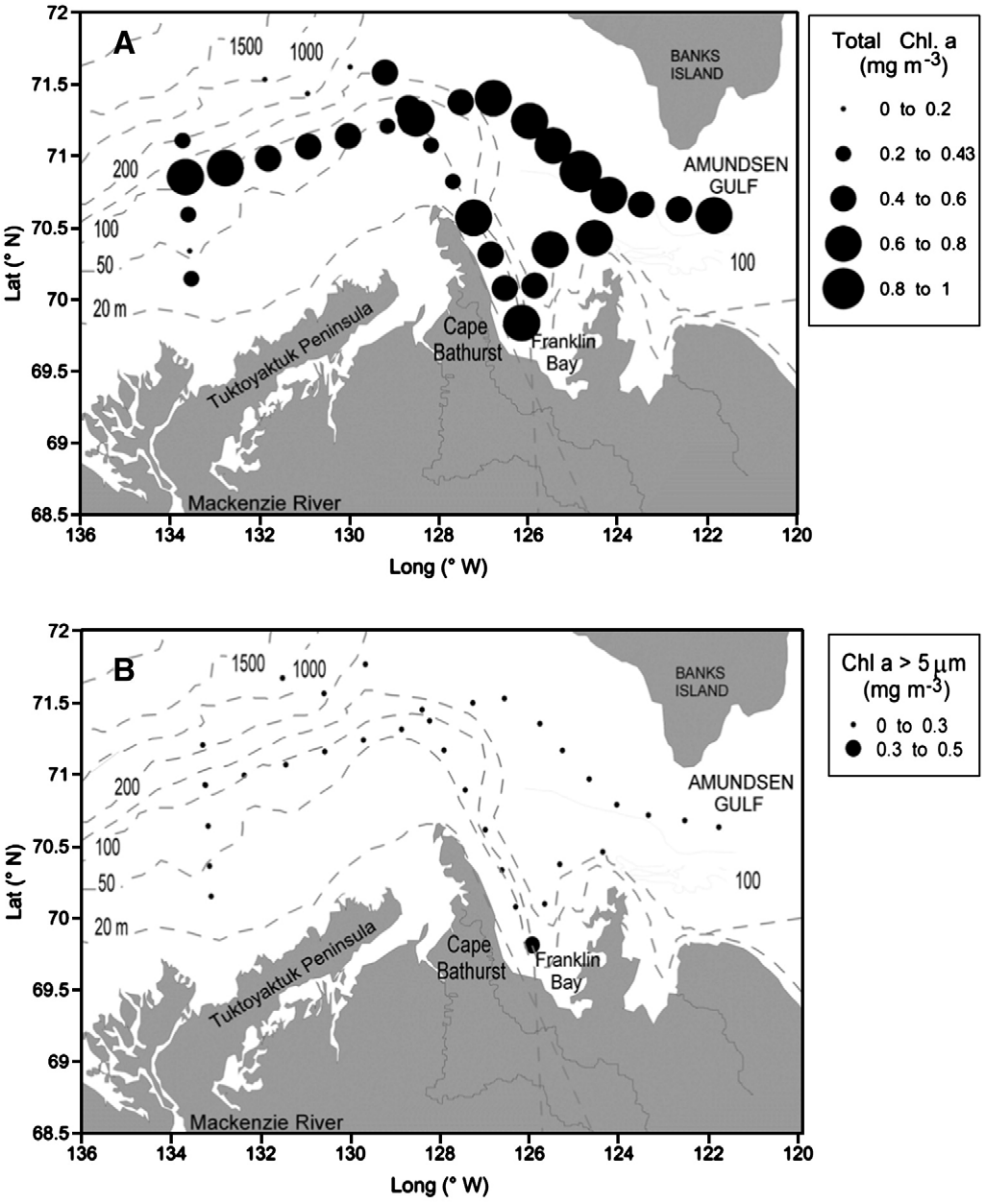

Fig. 5. A) Surface (0–10 m) average total (i.e., non-fractionated) Chlorophyll-*a* concentration at each station; B) Surface (0–10 m) average Chl *a* >5 μm.

with low-salinity and warm-temperature waters, highest picophytoplankton cell concentrations were found in Stns 59, 62 and 110, with 13810, 10240 and 10213 cells mL^{-1}, respectively (Fig. 6A). The lowest picophytoplankton abundances were found in the vicinities of Amundsen Gulf, in Stns 104 and 98, with less than 1500 cells mL^{-1}, contrasting with the high values found in Stn 110, to the east of these Stns. On average in the area, picophytoplankton represented 71% of total cells (<20 μm). Three populations could be identified, the smallest of which was by far the most abundant one (81% of total picophytoplankton on average for all stations and depths). It dominated in all stations but in the surface of Stn 42 and in Stns 45, 49 and 53. There, a second, slightly larger population dominated the picophytoplankton assemblage. Nanophytoplankton concentrations varied between 3 and 2901 cells mL^{-1} (average=570±39 cells mL^{-1}). Maximum cell concentrations were found in surface waters of Stns 59 and 62 (2901 and 2850 cells mL^{-1}, respectively, Fig. 6B), in the area of influence of the Mackenzie River. At all but Stns 21 and 98, nanophytoplankton cells' size was <10 μm (Fig. 6B). Nanophytoplankton >10 μm cell concentrations were generally <100 cells mL^{-1}.

The photochemical quantum yield Fv/Fm, a proxy measurement for photosynthetic efficiency of algae or health condition of PSII, averaged 0.44 (±0.14) for all stations and depths. In most cases, maximum Fv/Fm was found very close to the surface (i.e., at depths <10 m) and mostly did not coincide with maximum total phytoplankton concentrations. To further study the variability in Fv/Fm, together with Chl *a*, picophytoplankton and nanophytoplankton concentrations, data were pooled according to the sampling time (four intervals were chosen: from 06:00 to 10:00, from 10:00 to 14:00, from 14:00 to 18:00 and from 18:00 to 6:00 h) and the depth of

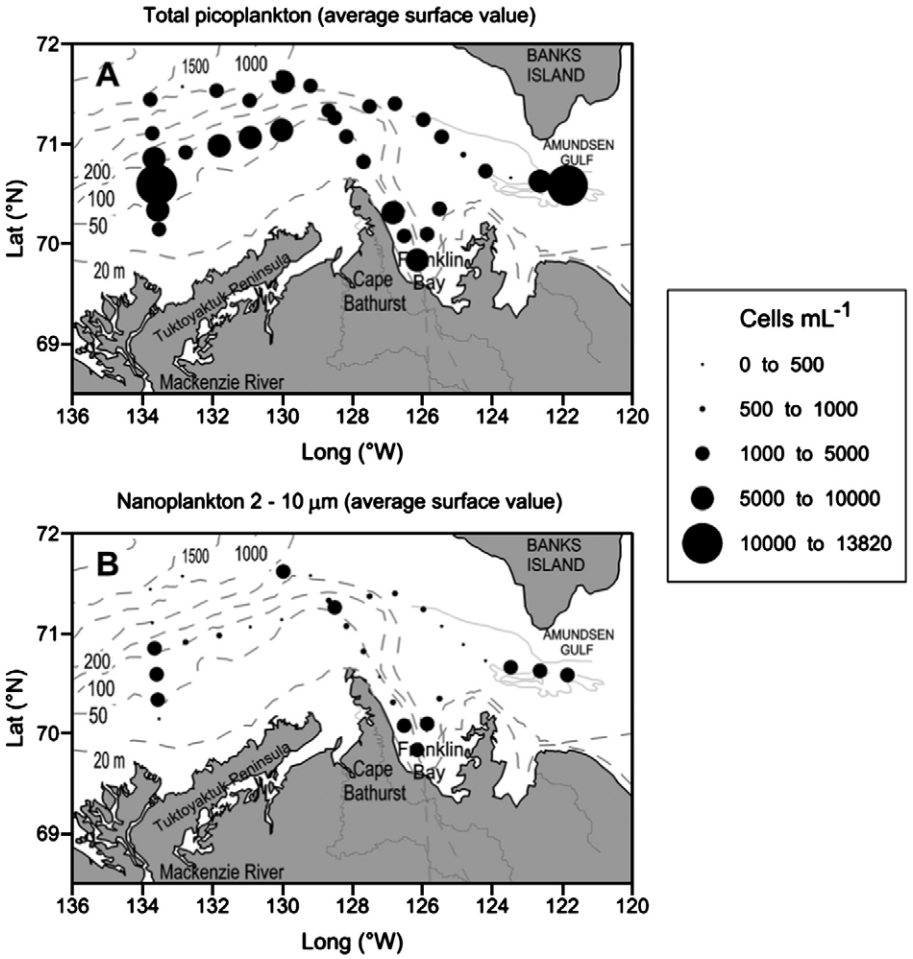

Fig. 6. Distribution of surface (0–10 m) average phytoplankton cell number (<20 μm) in each station. A) Picophytoplankton, B) Nanophytoplankton <10 μm.

sampling (samples at depths <10 m, between 10 and 50 m and at depths >50 m). Significant differences in Fv/Fm were found between the samples taken at midday (between 10 and 14 h), those taken between 14 and 18 h and those from 18 to 6 h, the highest value being for the midday sample, under maximum environmental light conditions (ANOVA, $p<0.05$; Fig. 7). No significant differences were found for Chl *a*, picophytoplankton and nanophytoplankton distribution for the different sampling hours (not shown, ANOVA, $p=0.33$). In addition, surface samples (<10 m) showed significantly higher Fv/Fm ratios ($p<0.05$) than intermediate depths (10 to 50 m). This was accompanied by significantly higher Chl *a* and cell numbers ($p<0.05$) at samples from depth <10 m (data not shown).

In order to show the vertical distribution of some of the parameters (salinity, Chl *a*, phytoplankton <20 μm, and Fv/Fm) four stations have been chosen (Fig. 8). Both Stns 49 and 65 have been chosen to allow the comparison with other variables that have been studied by other authors: picocyanobacteria distribution (Galand et al., 2006), CDOM optical properties (Retamal et al., 2007), prokaryotic community structure and heterotrophic production (Garneau et al., 2006). In addition, Archaean distribution (Wells et al., 2006; Waleron et al., 2007), microbial eukaryotes (Lovejoy et al., 2006) and picoprasinophytes were studied for Stn 65. Stn 66 was also characterised by Garneau et al. (2006). Finally, Stn 107 was chosen since it contains some of the highest numbers of cells measured. On the outer Mackenzie Shelf and the ice edge zone (Stn 49), the waters above 60 m were salinity stratified. Phytoplankton (<20 μm) and Chl *a* concentrations were at their highest concentrations at 60 m depth, where the highest Fv/Fm was also determined. Warm and deep Atlantic waters are evident in temperature (not shown), below 200 m depth. At the plume of the Mackenzie River (Stn 66), the highest phytoplankton (<20 μm) abundance was found in surface waters, but Chl *a* concentrations were very low. Fv/Fm was also low in surface waters but increased with depth and salinity. Although Stn 66 was located farther from the Mackenzie River mouth than Stn 65, a salinity minimum was observed in Stn 66. A relative increase in both Chl *a* and phytoplankton (<20 μm) abundance was evident in surface waters, although Fv/Fm was lower in surface (<10 m) than between 20 and 40 m. An increase in biomass and photosynthetic activity was evident close to the bottom of the station. In the vicinity of Amundsen Gulf (Stn 107) maximum phytoplankton (<20 μm), Chl *a* concentrations and Fv/Fm were found above the halocline, in waters influenced by ice melt. Below the halocline, in waters presenting characteristics common with the Winter Mixed Layer, both Chl *a* concentration and phytoplankton abundance (<20 μm) were low.

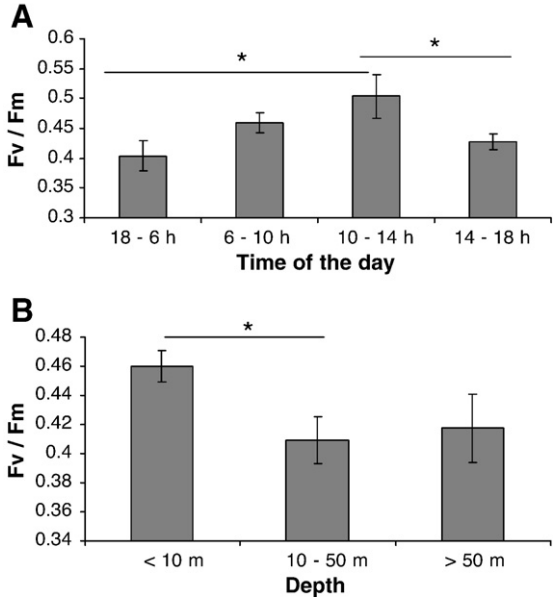

Fig. 7. Results of the ANOVA's contrasting the Fv/Fm ratio for different times of the day (A) and different depth intervals (B). The lines and the asterisks over the lines indicate that significant differences were found among groups.

Spearman rank correlations performed on environmental and biological data from the same 3 depth ranges analysed (<10 m, between 10 and 50 m, and >50 m; Table 1) revealed that, except for the exhausted nitrate+nitrite in surface waters, mainly salinity but also temperature for depths >10 m are significantly related to the distribution of nutrients at all depths ($p<0.01$). In both surface (<10 m) and deep waters (>50 m), the salinity shows significant negative correlations with picophytoplankton and nanophytoplankton abundances ($p<0.01$). In intermediate waters, salinity was only correlated to picophytoplankton abundance. Furthermore, the photochemical quantum yield Fv/Fm was significantly correlated only to total Chl *a* in surface waters ($p<0.001$) and to phosphate concentration at depths >50 m ($p<0.05$).

4. Discussion

Few regional-scale biological studies have been carried out in the Canadian Beaufort Sea (cf. Parsons et al., 1988, 1989; Carmack et al., 2004). The autumn season, for which very little information is available, can be depicted on arctic shelves as a transition from a system characterised by the presence of ice melt and river water in the surface layer to one in which the upper

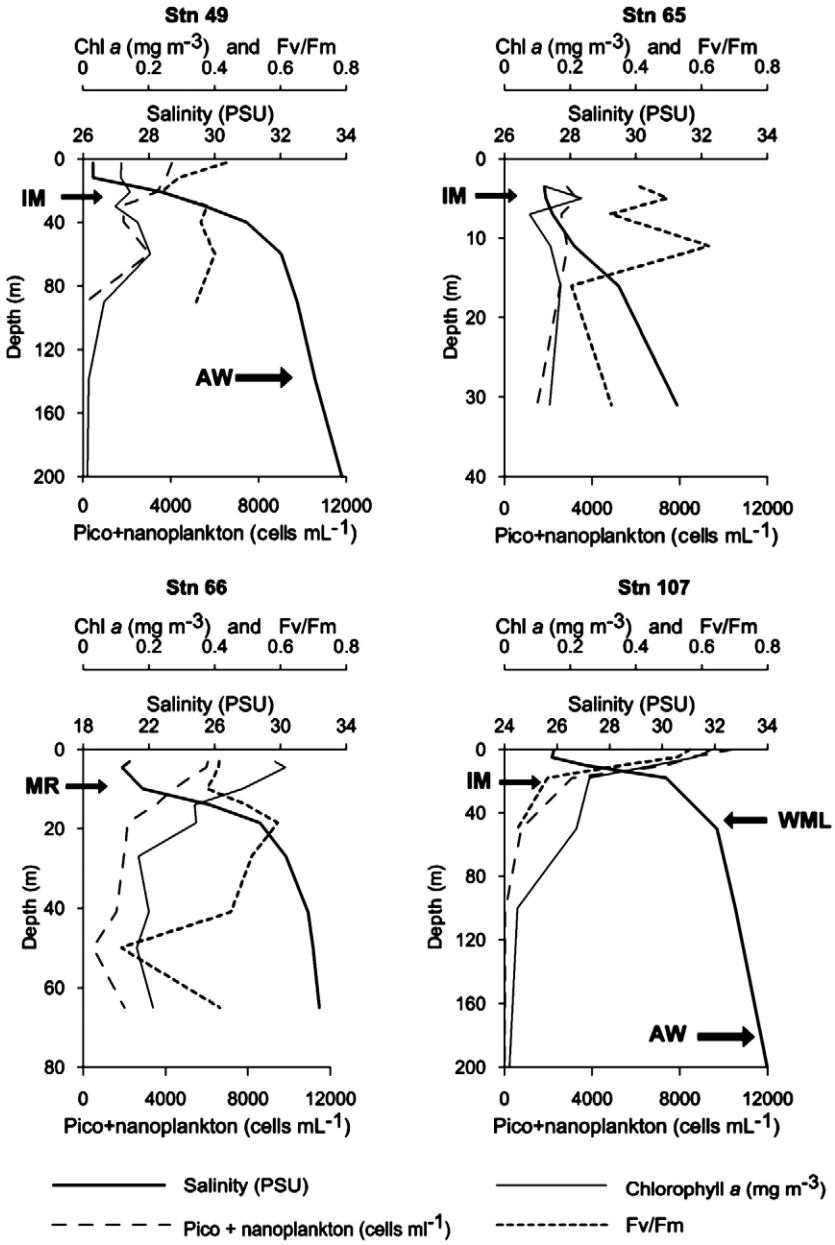

Fig. 8. Selected stations representing the different sectors of the study area as defined in Fig. 2, to show the vertical distribution of salinity, phytoplankton <20 μm, Chl *a* and Fv/Fm.

waters are strongly mixed by the winds until freezing starts, usually in mid-October (Carmack and Macdonald, 2002). As such, phytoplankton cells are likely to be trapped in the newly formed frazil ice. Ice algae (as well as small flagellates) can significantly contribute to the total biomass present in the ice (Gradinger, 1999). Such trapped cells could then potentially survive the winter and seed the water column during the following spring, as has been described for Antarctic sea ice algae (Lizotte, 2001). Therefore, phytoplankton composition and relationships with water masses and ice characteristics during fall greatly influence the structure of the entire trophic web and the system's fluxes and export of carbon.

4.1. Characterisation of the water masses according to phytoplankton (<20 μm) cell abundances

The different water masses described in previous studies in the Canadian Arctic Shelf (see Carmack et al.,

Table 1
Spearman rank correlations performed on environmental and biological data from 3 different depth ranges

	Salinity	Chl *a*	Picophytoplankton	Nanophytoplankton	NO_3+NO_2	PO_4	SiO_4	Fv/Fm
Depth<10 m								
Temperature	**−0.56**	−0.09	0.17	−0.13	**0.04**	−0.44	0.09	−0.02
Salinity		**−0.34**	−0.44	−0.22	0.10	**0.67**	**−0.50**	0.13
Chl *a*			0.15	0.08	**0.30**	−0.23	**0.41**	**0.31**
Picophytoplankton				**0.48**	0.01	−0.26	**0.33**	−0.10
Nanophytoplankton					0.09	−0.22	**0.29**	−0.03
NO_3+NO_2						0.16	**−0.02**	0.23
PO_4							−0.41	0.00
SiO_4								0.09
Depth>10 m and <50 m								
Temperature	**−0.55**	0.26	0.04	0.03	**−0.56**	**−0.60**	**−0.51**	0.14
Salinity		−0.22	**−0.54**	0.12	**0.75**	**0.75**	**0.70**	−0.31
Chl *a*			0.13	0.31	−0.06	−0.08	−0.05	0.03
Picophytoplankton				−0.17	**−0.33**	−0.30	−0.32	0.15
Nanophytoplankton					0.21	0.11	0.27	−0.19
NO_3+NO_2						**0.69**	**0.78**	**−0.33**
PO_4							**0.64**	−0.22
SiO_4								−0.21
Depth>50 m								
Temperature	−0.25	0.06	0.27	0.25	−0.29	**−0.39**	**−0.47**	0.06
Salinity		**−0.82**	**−0.70**	**−0.63**	**0.73**	**0.44**	**0.52**	−0.07
Chl *a*			**0.67**	**0.67**	**−0.49**	−0.27	−0.27	0.18
Picophytoplankton				**0.69**	**−0.41**	**−0.40**	−0.31	0.18
Nanophytoplankton					−0.24	−0.37	−0.30	0.21
NO_3+NO_2						**0.52**	**0.71**	−0.10
PO_4							**0.59**	−0.33
SiO_4								−0.12

Underlined values denote $p<0.05$, bold values, $p<0.01$; bold and underlined ones, $p<0.001$.

2004) were identified during the present study. One environmental variable – salinity – was especially well correlated with most of the measured variables (Table 1) such as nutrients, phytoplankton abundances (i.e. Chl *a*) and the most abundant phytoplankton group (i.e., picophytoplankton), especially in surface waters. To allow formal comparison with water mass distributions, phytoplankton cell abundances (<20 μm) were plotted as a function of temperature and salinity; the different water masses identified in the area (see Fig. 2) were indicated on the diagram (Fig. 9). Differences among the so defined water masses were then examined for Chl *a* concentration, picophytoplankton and nanophytoplankton cell number, and Fv/Fm. A synthesis of the characteristics of the different regions is presented in Table 2. Significant differences for the biological parameters analysed among water masses were evident (ANOVA, $p<0.05$, Table 2). Post-hoc comparisons evidenced that significant differences ($p<0.05$) among regions were found mainly when comparing picophytoplankton cell concentrations. Although picophytoplankton abundance in IM waters was only half of that found in the MR plume (where maximum cell concentrations were found) they were still significantly higher than cell concentrations in all the other water masses. WML was significantly different from PWW for picophytoplankton cell abundance. The MR plume also showed significantly higher abundances of nanophytoplankton cells. Differences in this group's abundance were also evident between the IM and the PWW. Chl *a* concentrations were significantly higher ($p<0.05$) in the IM than in any other water mass. There were no significant differences in Chl *a* concentration among the other water mass. Notably, no significant differences in the Fv/Fm ratio among water masses were found. The above results allow concluding that the various water masses present in the Beaufort Sea are characterised by distinct ranges of pico- and nanophytoplankton abundances. This is not surprising for the deep AW, but still holds true for surface waters (MR, IM) as well as for the PWW. A similar conclusion was reported by Mostajir et al. (2001) who were able to distinguish the origin of two different surface water masses in the northern Baffin Bay region based on picophytoplankton abundance.

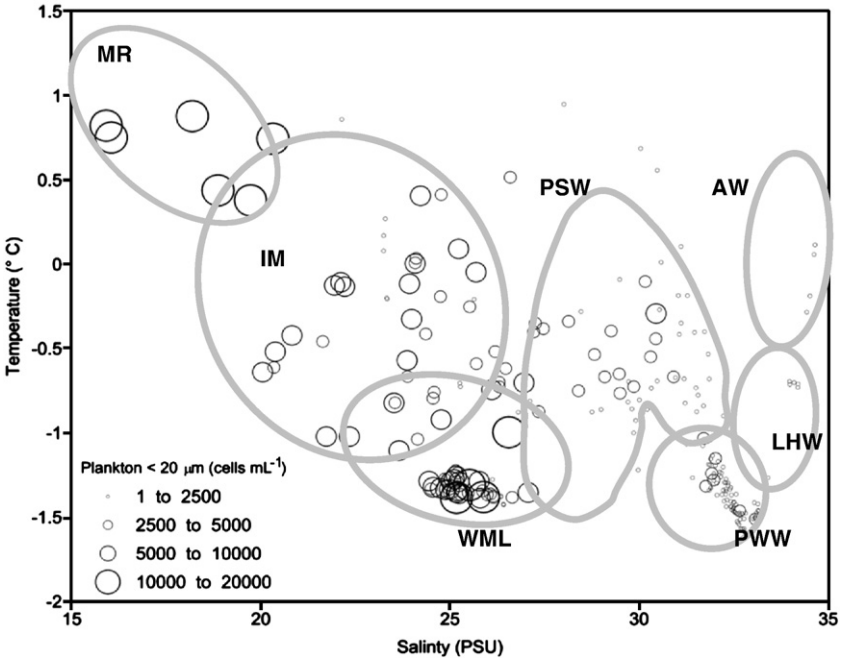

Fig. 9. Distribution of phytoplankton <20 µm cell number as a function of temperature and salinity; the different water masses identified in the area (see Fig. 2) are indicated on the figure: MR is Mackenzie River; IM is ice melt water; WML is the Winter Mixed Layer; PSW is Pacific Summer Water; PWW is Pacific Winter Water; LHW is Lower Halocline Water; and AW is Atlantic Water.

4.2. Size structure of phytoplankton <20 µm assemblages

High picophytoplankton and low nanophytoplankton abundances were evident in all the water masses defined for the area. In general, Chl *a* <5 µm represented ca. 70% of total phytoplankton biomass. Furthermore, considering all data, Spearman rank correlations evidenced that Chl *a* was significantly ($r=0.55$; $p<0.05$) correlated with total <20 µm (picophytoplankton + nanophytoplankton) cell concentration. This high correlation is produced by picophytoplankton abundance ($r=0.56$; $p<0.05$), while no significant correlation was found for nanophytoplankton ($p=0.12$). Therefore, although no information is available on phytoplankton >20 µm, it could be concluded that picophytoplankton dominated the total phytoplankton community at all studied stations. Similar results have been shown for other areas in the Arctic Ocean (Booth and Horner, 1997; Mostajir et al., 2001; Vidussi et al., 2004; Not et al., 2005). It is hypothesised that in the present study, the species responsible for the picophytoplankton peak could probably be the prasinophyte *Micromonas* sp., whose occurrence has been frequently reported in the Arctic Ocean (Throndsen, 1970; Sherr et al., 2003; Not et al., 2005; Lovejoy et al., 2007) and which has been found in ice-free areas, when nitrate concentrations were low (Booth and Smith, 1997). This species is also reported in estuarine environments at lower latitudes (Ansotegui et al., 2003).

4.2.1. Phytoplankton <20 µm and freshwater inputs in the SE Beaufort Sea

The Mackenzie River, the largest North American source of freshwater for the Arctic Ocean (Stewart et al., 1998), carries large amounts of inorganic and organic matter into the Arctic Ocean, including living biota (Garneau et al., 2006). These particle-rich waters first spread across the coastal Mackenzie Shelf before being transported by wind and buoyancy-driven surface currents over the shelf. The high picophytoplankton concentrations found in the MR plume and in IM waters along the Mackenzie Shelf (which contain lower but still high amounts of phytoplankton cells) confirm the potential importance of the MR as a source of phytoplankton cells (<20 µm) to the whole area (see 4.2). Freshwater inputs are very often accompanied by phytoplankton cells (<20 µm) as evidenced in the high picophytoplankton abundances found in low-salinity waters and in the correlation between salinity and nanophytoplankton cells in surface waters during the present study. Similar results where obtained by Waleron et al. (2007) for epifluorescence cell counts. These authors showed that picocyanobacteria present in the coastal Arctic

Table 2
Mean and standard errors of some physical and biological variables in the different water masses found in the CASES study area during fall 2002, according to Fig. 2

	Temperature (°C)		Salinity (PSU) (mg m^{-3})		N	Chl. *a* Picophytoplankton (cells mL^{-1})			Nanophytoplankton		N	Fv/Fm		N
	Average	Standard error	Average	Standard error		Average	Standard error	Average	Standard error			Average	Standard error	
1 – MR	**0.67**	0.09	**18.17**	0.76	6	0.10	0.04	**9259**	405	**2209**	518	4	0.44	0.01	4
2 – IM	−0.87^{4}	0.06	**24.78**	0.18	88	**0.50**	0.02	**4169**	263	769^{5}	53	79	0.46	0.01	77
3 – WML	−0.69^{5}	0.05	**29.27**	0.21	31	0.18	0.02	2033^{5}	183	471	112	28	0.44	0.01	28
4 – PSW	−0.44^{2,5}	0.07	**31.21**	0.13	21	0.19	0.01	888	134	572	117	19	0.39	0.02	17
5 – PWW	−1.36^{3}	0.02	**32.38**	0.05	83	0.11	0.01	575^{3}	95	304^{2}	49	67	0.40	0.02	54
6 – AW	−0.43	0.12	**34.30**	0.09	9	0.01	0.00	303	290	209	189	5	0.51	0.11	3
7 – Nonld	**0.66**	0.00	**27.01**	0.00	6	0.25	0.00	1949	0	561	0	5	0.48	0.03	5
All Groups	−0.88	0.04	28.73	0.26	244	0.28	0.02	2367	170	569	39	207	0.14	0.01	1

RP: Mackenzie River Plume; SML: Surface Mixed Layer; WW: Winter Waters; PSW: Pacific Surface Water; PWW: Pacific winter water; AW: Atlantic water. 7-Nonld: non identified waters; waters not associated with any of the above described waters. Bold numbers indicate that for a certain variable significant differences were found between a certain characteristic of a given water mass and all the others in Post-hoc comparisons of the ANOVA. Underlined values indicate that significant differences were evident from the Post-hoc tests only between the variable underlined in a certain region and a second one, which is indicated as an exponent. *N* indicates the number of stations considered.

Ocean could be of riverine origin. However, for other planktonic groups such as Archaea (Galand et al., 2006) and microbial eukaryotes (Lovejoy et al., 2006), a community change between the river and the adjacent sea is evident. This stresses the importance of detailed taxonomic studies in the characterisation of arctic microbial communities. In some of these works a group of stations (Stns 65, 66 and 49, Fig. 1; Fig. 8) corresponding to a transect perpendicular to the coast, starting close to MR mouth was analysed to follow the influence of the MR on the Beaufort shelf. Stn 66, which is located in the middle of this transect, was characterised by the highest surface temperature and the lowest surface salinities (Fig. 8), a high proportion of picocyanobacteria (Waleron et al., 2007), Archaea concentration (Wells et al., 2006), and the presence of β-proteobacteria (Garneau et al., 2006), which are all characteristic of riverine waters. The latter authors suggested that the presence of these waters in an intermediate station had its origin in the waters flowing from the main river channel at the western side of the MR mouth, later deflected eastward, 150 km offshore (Garneau et al., 2006). Both Stns 65 and 49 showed evidence of less fresh water influence than Stn 66. In fact, two other intermediate stations, Stn 59 and to a lesser extent Stn 62, which were not considered in neither of the mentioned studies, showed even higher temperatures and lower salinities in surface waters than Stn 66, as well as the highest picophytoplankton abundance ($>1.3\times10^{4}$ cells mL^{-1}). This suggests that the freshwater flow had an extension of ~50 km, with its core some 120 km offshore. Unfortunately, information on the taxonomic composition of the dominating picophytoplankton group at Stns 59 and 62 is not available, although a dominance by picocyanobacteria such as found in Stn 66 by Waleron et al. (2007) could be expected; the same population of picophytoplankton represented almost 100% of picophytoplankton cells in all three stations.

River runoff and sea ice melt greatly reduce surface water salinities. In coastal Antarctic environments, meltwater has been shown to favour the development of a group of phytoflagellates, the Cryptomonads over diatoms (Moline et al., 2004). Although these results could not be confirmed by Garibotti et al. (2005), such a change could in turn affect the abundance of herbivorous plankton, thus altering the entire food web. A similar response might be expected for the arctic shelves.

4.2.2. The central Beaufort Sea and Amundsen Gulf waters

In Stns 33 to 49 at the shelf break, where depths exceeded 200 m (and where the influence of Atlantic

waters is shown by the higher temperatures and salinities), very low amounts of picophytoplankton cells were found and phytoplankton <20 μm was dominated by nanophytoplankton <10 μm. The characteristics of the surface waters in these stations are similar to those in the western part of the coastal transect between Stns 66 and 89 probably due to time elapsed between the two parallel to the coast transects, which could have allowed the pack ice to extend southward. However, maximum picophytoplankton concentrations in the surface waters of the first transect varied between 3900 and 5500 cells mL^{-1}, while for the last one they varied between 3800 and 8500 cells mL^{-1}. These slightly higher values were likely related to enhanced phytoplankton growth favoured by increased water column stability closer to the coast (data not shown). Waters of terrestrial origin around Franklin Bay could additionally contribute to phytoplankton cell concentrations in the area. Cells might then again be diluted eastward by the effect of the winds. During the first 10 days of this study winds came dominantly from the East during (Environment Canada, 2002).

In Amundsen Gulf, total phytoplankton (<20 μm) abundance was highest in the surface waters at Stns 107 (Fig. 8) and 110, dominated by picophytoplankton. Their concentration was twice that described by Waleron et al. (2007) for the neighbour Stn 101 at 5 m. The dominance of small cells in the area was previously described by Lee and Whitledge (2005) for summer 2002, who further described this area as the most productive area in the Canadian Basin (Lee and Whitledge, 2005).

4.3. The physiological state of phytoplankton in the SE Beaufort Sea during fall

The lack of variability found when comparing Fv/Fm for the different water masses described would indicate that growth conditions are similar all over the study area or that organisms were acclimated to growing in the different conditions encountered. The values of the Fv/Fm ratio indicate that phytoplankton were still active. Photosynthesis would not be inhibited by midday or surface waters light. Primary production measurements at several stations (Stns 24, 49, 65, 66, 83 and 101) during the same period showed that maximum daily production rates occur in surface waters (depth <10 m) (S. Brugel et al., in prep), thereby supporting the present interpretation. Our findings additionally indicate that light might have been a limiting factor rather than a photoinhibiting factor for phytoplankton to develop at depths >10 m. Moreover, there was a small (ca. 20%) decrease in night Fv/Fm values. In the tropical Pacific Ocean Behrenfeld et al. (2006) found a pattern similar to our, with nocturnal decreases in Fv/Fm. They divided their study area in 4 regimes according to the degree of nocturnal decrease and down increase in Fv/Fm. Our findings would fit in their regime I (percentage decrease in Fv/Fm <25%; dawn normalized variable fluorescence Fv/Fm ≥0.45), which corresponded to oligotrophic, iron sufficient and low-nutrient concentration waters. Although iron concentration was not measured during CASES 2002, we assume that no iron limitation will occur in shallow coastal areas; nutrient concentrations were on occasions undetectable or very low, so that the conditions would be similar to those described by Behrenfeld et al. (2006).

The fact that the highest Fv/Fm values were found in the surface waters suggests that phytoplankton would not be affected by nutrient limitation in the present study. Moreover, phytoplankton cells could be growing on ammonium, which is their preferred nitrogen species for growth (Wheeler and Kirchman, 1986; Harrison and Wood, 1988). Ammonium data are not available for the present study. The low macronutrient (especially nitrate) concentrations measured during the present study could result from dilution by freshwater input. Nitrate was probably the limiting nutrient for >20 μm phytoplankton growth, as evidenced by the low N:P ratio calculated, and as previously described for the Beaufort Sea (Carmack and Macdonald, 2002; Carmack et al., 2004; Lovejoy et al., 2006). Silicate concentrations were significantly and negatively correlated to salinity in surface waters (Table 1). Silicate could be supplied by the low-salinity Mackenzie River waters (Carmack and Macdonald, 2002). At depth, silicates as well as the other analysed macronutrients were probably not consumed by phytoplankton at this time of the year.

In summary, our work establishes a relationship between water masses physical characteristics (salinity and temperature) and phytoplankton <20 μm abundance. The composition and abundance of phytoplankton are of central importance to the structure and functioning of the trophic webs and to the carbon transfer in the arctic ecosystem. Understanding the actual link between physics and biology is a first step in the prediction of the response of the system to climate change. Global circulation models further predict a warming of Mackenzie River waters of about ~4.2 °C for the next 20 years (Nijssen et al., 2001). Since most of the precipitation in the Mackenzie Basin is stored as snow, spring snowmelt runoff is predicted to increase in a warming scenario (Nijssen et al., 2001). With the freshwater runoff increase that is expected to enter the Arctic Shelves (Peterson et al., 2002), the impact

particle size and its effects on biological communities remains a central question.

Acknowledgements

This research, as part of the Canadian Arctic Shelf Exchange Study (CASES), was supported by grants from the Natural Sciences and Engineering Research Council (NSERC) of Canada to S.D. We thank Karine Lacoste and Gitane Caron for Chl *a* analyses, Coralie Furon and Gervais Ouellet for flow cytometry analyses, and Simon Bélanger for fruitful discussions. We are grateful to Louis Fortier for his dedication as leader of the CASES project and to Martin Fortier, chief scientist during CASES 2002. We are also grateful to the Canadian Coast Guard officers and crews of the ice-breaker 'Pierre Radisson' for their skilful support during the expedition.

References

Ansotegui, A., Sarobe, A., Trigueros, J.M., Urrutxurtu, I., Orive, E., 2003. Size distribution of algal pigments and phytoplankton assemblages in a coastal–estuarine environment: contribution of small eukaryotic algae. J. Plankton Res. 25, 341–355.

Barber, D.G., Hanesiak, J., 2004. Meteorological forcing of sea ice concentrations in the southern Beaufort Sea over the period 1978 to 2001. J. Geophys. Res. 109, C06014. doi:10.1029/2003JC002027.

Behrenfeld, M.J., Worthington, K., Sherrell, R.M., Chavez, F., Strutton, P., McPhaden, M., Shea, D., 2006. Controls on tropical Pacific Ocean productivity revealed through nutrient stress diagnostics. Nature 442, 1025–1028.

Booth, B.C., Horner, R.A., 1997. Microalgae on the Arctic Ocean Section, 1994: species abundance and biomass. Deep-Sea Res. II 44, 1607–1622.

Booth, B.C., Smith Jr., W.O., 1997. Autotrophic flagellates and diatoms in the Northeast Water Polynya, Greenland: summer 1993. J. Mar. Syst. 10, 241–261.

Carmack, E.C., Macdonald, R.W., 2002. Oceanography of the Canadian Shelf of the Beaufort Sea: a setting for Marine Life. Arctic 56, 29–45.

Carmack, E.C., Macdonald, R.W., Jasper, S., 2004. Phytoplankton productivity on the Canadian Shelf of the Beaufort Sea. Mar. Ecol., Prog. Ser. 277, 37–50.

Carmack, E.C., Barber, J.C., Macdonald, R.W., Rudels, B., Sakshaug, E., 2006. Structure and function of contemporary food webs on Arctic shelves: a pan-Arctic comparison. Prog. Oceanogr. 71, 145–181.

Environment Canada, 2002. Archives nationales d'information et de données climatologiques. At: www.climat.meteo.ec.gc.ca/climateData/canada_f.html.

Falkowski, P.G., Raven, J.A., 1997. Aquatic Photosynthesis. Blackwell Science. 375p.

Galand, P.E., Lovejoy, C., Vincent, W.F., 2006. Remarkably diverse and contrasting archaeal communities in a large arctic river and the coastal Arctic Ocean. Aquat. Microb. Ecol. 40, 11–126.

Garibotti, I.A., Vernet, M., Ferrario, M., 2005. Annually recurrent phytoplanktonic assemblages during summer in the seasonal ice zone west of the Antarctic Peninsula (Southern Ocean). Deep-Sea Res. I 52, 1823–1841.

Garneau, M.E., Vincent, W.F., Alonso-Sáez, L., Gratton, Y., Lovejoy, C., 2006. Prokaryotic community structure and heterotrophic production in a river-influenced coastal arctic ecosystem. Aquat. Microb. Ecol. 42, 27–40.

Gradinger, R., 1999. Vertical fine structure of algal biomass and composition in Arctic pack ice. Mar. Biol. 133, 745–754.

Grasshoff, K., 1999. Methods of Seawater Analyses. Weinheim, New Yord. 600 p.

Harrison, W.G., Wood, L.J.E., 1988. Inorganic nitrogen uptake by marine picophytoplankton: evidence for size partitioning. Limnol. Oceanogr. 33, 468–475.

Kirk, J.T.O., 1983. Light and Photosynthesis in Aquatic Ecosystems. Cambridge University Press, Cambridge. 401 pp.

Koenings, J.P., Edmundson, J.A., 1991. Secchi disk and photometer estimates of light regimes in Alaskan lakes: effects of yellow color and turbidity. Limnol. Oceanogr. 36, 91–105.

Lee, S.H., Whitledge, T.E., 2005. Primary and new production in the deep Canada Basin during summer 2002. Polar Biol. 28, 190–197.

Lizotte, M.P., 2001. The contributions of sea ice algae to Antarctic marine primary production. Am. Zool. 41, 57–73.

Lovejoy, C., Massana, R., Pedrós-Alió, C., 2006. Diversity and distribution of marine microbial eukaryotes in the Arctic Ocean and adjacent seas. Appl. Environ. Microb. 72, 3085–3095.

Lovejoy, C., Vincent, W.F., Bonilla, S., Roy, S., Martineau, M.-J., Terrado, R., Potvin, M., Massana, R., Pedrós-Alió, C., 2007. Distribution, phylogeny and growth of cold-adapted picoprasinophytes in arctic seas. J. Phycol. 43, 78–89. doi:10.1111/j.1529-8817.2006.310.x.

Macdonald, R.W., Carmack, E.C., Mclaughlin, F.A., Iseki, K., Macdonald, D.M., O'brien, M.O., 1989. Composition and modification of water masses in the Mackenzie Shelf Estuary. J. Geophys. Res. 94, 18057–18070.

McLaughlin, F.A., Carmack, E.C., Macdonald, R.W., 1996. Physical and geochemical properties across the Atlantic/Pacific water mass front in the southern Canadian Basin. J. Geophys. Res. 101, 1183–1197.

McLaughlin, F.A., Carmack, E.C., Macdonald, R.W., Melling, H., Swift, J.H., Wheeler, P.A., Sherr, B.F., Sherr, E.B., 2004. The juxtaposition of Atlantic and Pacific-origin waters in the Canada Basin, 1997–1998: a basin in transition. Deep-Sea Res. I 51, 107–128.

Moline, M.A., Claustre, H., Frazer, T.K., Schofield, O., Vernet, M., 2004. Alteration of the food web along the Antarctic Peninsula in response to a regional warming trend. Glob. Change Biol. 10, 1973. doi:10.1111/j.1365-2486.2004.00825.

Mostajir, B., Gosselin, M., Gratton, Y., Booth, B., Vasseur, C., Garneau, M.-È., Fouilland, É., Vidussi, F., Demers, S., 2001. Surface water distribution of pico- and nanophytoplankton in relation to two distinctive water masses in the North Water, northern Baffin Bay, during fall. Aquat. Microb. Ecol. 23, 205–212.

Nijssen, B., O'Donnell, G.M., Hamlet, A.F., Lettenmaier, D.P., 2001. Hydrologic sensitivity of global rivers to climate change. Clim. Change 50, 143–175.

Not, F., Massana, R., Latasa, M., Marie, D., et al., 2005. Late summer community composition and abundance of photosynthetic picoeukaryotes in Norwegian and Barents Seas. Limnol. Oceanogr. 50, 1677–1686.

Parkinson, C.L., Cavalieri, D.J., Gloersen, P., Zwally, H.J., Comiso, J.C., 1999. Arctic sea ice extents, areas and trends, 1978–1996. J. Geophys. Res. 104, 20837–20856.

Parsons, T.R., Maita, Y., Lalli, C.M., 1984. A Manual of Chemical and Biological Methods for Seawater Analysis. Pergamon Press, Oxford. 173 pp.

Parsons, T.R., Webb, D.G., Dovey, H., Haigh, R., Lawrence, M., Hopky, G., 1988. Production studies in the Mackenzie River-Beaufort Sea estuary. Polar Biol. 8, 235–239.

Parsons, T.R., Webb, D.G., Rokeby, B.E., Lawrence, M., Hopky, G.E., Chiperzak, D.B., 1989. Autotrophic and heterotrophic production in the Mackenzie River/Beaufort Sea estuary. Polar Biol. 9, 261–266.

Peterson, B.J., Holmes, R.M., McClelland, J.W., Vorosmarty, C.J., Lammers, R.B., Shiklomanov, A.I., Rahmstorf, S., 2002. Increasing river discharge to the Arctic Ocean. Science 298, 2171–2173.

Peterson, B.J., McClelland, J., Curry, R., Holmes, R.N., Walsh, J.E., Aagaard, K., 2006. Trajectory shifts in the Arctic and Subarctic freshwater cycle. Science 313, 1061–1066.

Retamal, L., Vincent, W.F., Martineau, C., Osburn, C.L., 2007. Comparison of the optical properties of dissolved organic matter in two river-influenced coastal regions of the Canadian Arctic. Estuar. Coast. Shelf Sci. 72, 261–272.

Sherr, E.B., Sherr, B.F., Wheeler, P.A., Thompson, K., 2003. Temporal and spatial variation in stocks of autotrophic and heterotrophic microbes in the upper water column of the central Arctic Ocean. Deep-Sea Res. I 50, 557–571.

Shimada, K., Kamoshida, T., Itoh, M., Nishino, S., Carmack, E.C., McLaughlin, F., Zimmermann, S., Proshutinsky, A., 2006. Pacific ocean inflow: influence on catastrophic reduction of sea ice cover in the Arctic Ocean. Geophys. Res. Lett. 33, L08605.

Stein, R., Macdonald, R.W. (Eds.), 2004. The Organic Carbon Cycle in the Arctic Ocean. Springer, Berlin, Germany. ISBN: 3-540-01153-6. XIX, 363 pp.

Stewart, R.E., Crawford, R.W., Leighton, H.G., Marsh, P., Strong, G.S., Moore, G.W.K., Ritchie, H., Rouse, W.R., Soulis, E.D., Kochtubajda, B., 1998. The Mackenzie GEWEX Study: the water and energy cycles of a major North American river basin. Bull. Am. Meteorol. Soc. 79, 2665–2684.

Stroeve, J.C., Fetterer, F., Knowles, K., Meier, W., Serreze, M., Arbetter, T., 2005. Tracking the Arctic's shrinking ice cover: another extreme September minimum in 2004. Geophys. Res. Lett. 32, L04501. doi:10.1029/2004GL021810.

Throndsen, J., 1970. Flagellates from Arctic waters. Nytt Mag. Bot. 17, 49–57.

Troussellier, M., Courties, C., Zettelmaier, Z., 1995. Flow cytometric analysis of coastal lagoon bacterioplankton and picophytoplankton: fixation and storage effects. Estuar. Coast. Shelf Sci. 40, 621–633.

Vidussi, F., Roy, S., Lovejoy, C., Gammelgaard, M., Thomsen, H.A., Booth, B., Tremblay, J.E., Mostajir, B., 2004. Spatial and temporal variability of the phytoplankton community structure in the North Water Polynya, investigated using pigment biomarkers. Can. J. Fish. Aquat. Sci. 61, 2038–2052.

Waleron, M., Waleron, K., Vincent, W.F., Wilmotte, A., 2007. Allochthonous inputs of riverine picocyanobacteria to coastal waters in the Arctic Ocean. FEMS Microbiol. Ecol. 59, 356–365.

Wells, L.E., Cordray, M., Bowerman, S., Miller, L.A., Vincent, W.F., Deming, J.W., 2006. Archaea in particle-rich waters of the Beaufort Shelf and Franklin Bay, Canadian Arctic: clues to an allochthonous origin? Limnol. Oceanogr. 51, 47–59.

Wheeler, P.A., Kirchman, D.L., 1986. Utilization of inorganic and organic nitrogen by bacteria in marine systems. Limnol. Oceanogr. 31, 998–1009.